Article

JOURNAL OF COMPOSITE MATERIALS

Journal of Composite Materials
0(0) 1–8

DOI: 10.1177/0021998312468186
jcm.sagepub.com
SAGE

Development and in vitro assessment of bioactive glass/polymer nanostructured composites with silver

A Vulpoi[1,2], V Simon[1], H Ylänen[2] and S Simon[1]

Abstract

Two composites consisting of non-woven poly-96L/4D-lactide copolymer meshes and a bioactive glass containing silver and silver free were obtained in polyvinyl-alcohol solutions by slurry dipping method under slow mechanical stirring. The development of hydroxyapatite type nanocrystals on samples surface in simulated body fluid proved for both composites the tendency for high level of bioactivity. Their antibacterial effect was evaluated against Gram-negative *Escherichia coli* and Gram-positive *Staphylococcus epidermidis*. Both composites showed inhibitory effect on bacterial growth, but only the composite with silver containing bioactive glass proved to have bactericidal effect. The AgCl nanocrystals and Ag_3PO_4 particles self-assembled on the surface of this composite proved the release of silver ions into simulated body fluid.

Keywords

Composite biomaterials, silver, in vitro bioactivity, antibacterial effect

Introduction

Tissue engineering aims to maintain, restore or improve tissue functions.[1,2] Development of composite materials comprising a biodegradable polymeric phase and a bioactive inorganic phase, such as bioactive glass, is seen as a promising approach for scaffold production especially with regard to bone tissue engineering.[3] In the past few years, increasing attention has been paid to composites of bioabsorbable or biostable polymers and bioceramics. Various approaches to the development of such composites are investigated worldwide. Usually bioceramics are combined with the bulk or porous polymer matrix either as fillers or as coatings.[4-10]

The gradual polymer degradation, ideally matching the rate of tissue regeneration, leaves the space conductive to tissue ingrowth and vascularisation and the bioactive phase, like bioactive glass should promote bone growth.[2,11]

Bioactive silicate glasses are able to stimulate ostegenesis as well as angiogenesis, and therefore, they exhibit unique properties that make them highly attractive for bone tissue engineering applications.[12] Several studies have shown that the introduction of Ag_2O into bioactive glass compositions minimises the probability of microbial contamination and does not negatively influence the glass matrix bioactivity.[13-15] On the other hand, delivering silver ions for antimicrobial utilization is arguable because silver ions are electrically attracted and rapidly form complexes or compounds wherein the ion is no longer available to perform the appropriate antimicrobial function.[16,17] It was also reported that the formation of Ag_3PO_4 affords tuneable Ag release rates and enhances the antibacterial activity by ions release in biological fluids.[18]

The present work was focused on development and characterisation of two composites consisting of non-woven poly-96 L/4D-lactide copolymer meshes and a bioactive glass with silver and free of silver. The bioactivity of the composites was tested in simulated body fluid (SBF). Their antibacterial effect was tested on *Escherichia coli* and *Staphylococcus epidermidis*.

[1]Faculty of Physics & Institute for Interdisciplinary Research on Bio-Nano-Sciences, Cluj-Napoca, Babes-Bolyai University, Romania
[2]Tampere University of Technology, Tampere, Finland

Corresponding author:
S Simon, Faculty of Physics & Institute for Interdisciplinary Research on Bio-Nano-Sciences, Cluj-Napoca, Babes-Bolyai University, M. Kogalniceanu 1, 400084, Romania
Email: simons@phys.ubbcluj.ro

Experimental

In order to obtain the polymer braiding, poly-96 L/4D-lactide (PLA) copolymer fibers were uniformly combed to a roll and a sheet of parallelly orientated fibers was obtained. The sheet was cut in two pieces which were overlaid with perpendicular orientation of the fibers. The two sheets assembly was processed with a device of pouncing needles that led to a pattern of non-woven meshes.

Bioactive glasses of $56SiO_2{\cdot}(40\text{-}x)CaO{\cdot}4P_2O_5{\cdot}xAg_2O$ system, with $x = 0$ (noted BG) and 4 mol% (noted AgBG), were prepared via sol-gel method as reported elsewhere.[19,20] The gels were aged for 7 days at room temperature, and thereafter the dried gels were heat-treated at 580°C for 1/2 h.

The obtained PLA meshes were coated with bioactive glass particles using slurry dipping method.[21] The slurry was formed from bioactive glass and 4% polyvinyl-alcohol (PVA) aqueous solutions; the ratio between PVA and bioactive glass was 40/60. Pieces of 10×10 mm of fabric were first pre-treated in ethanol for 30 min to improve wetability, washed with distilled water and dipped into the slurry using tweezers, and left immersed for 3 min under continuous slow steering to avoid precipitation of bioactive glass powder. After withdrawal, the samples were put on glass plates and every 2 min they were turned from one side to the other, for half an hour, then the composites were left to dry for 3 days at room temperature.The morphology of the composites was studied by scanning electron microscopy (SEM). Thermal analysis was used to quantify the bioactive glass content on the polymer meshes. The structure of the neat polymers and composite samples was investigated by X-ray diffraction (XRD).

Scanning electron microscopy (SEM) images were taken with an FEI Quanta 3D FEG 200/600 microscope equipped with energy dispersive X-ray spectrometer (EDS). In order to amplify the secondary electrons signal, the samples were sputter coated with platinum in an Agar automatic sputter coater. Chemical analysis of local area was carried out by EDS measurements performed on same microscope. Thermogravimetric (TG) measurements were carried on a Shimadzu analyzer DTG-60H from room temperature to 500°C, using alumina crucibles, with heating rate of 5°C/min. XRD patterns were recorded with a Shimadzu XRD-6000 diffractometer, using Cu K_α radiation ($\lambda = 1.5418$ Å), with Ni-filter. The samples were tested for bioactivity in SBF.[22]

The antibacterial effect of the composites was investigated on genetically modified light-emitting bacteria *Escherichia coli* and *Staphylococcus epidermidis* by

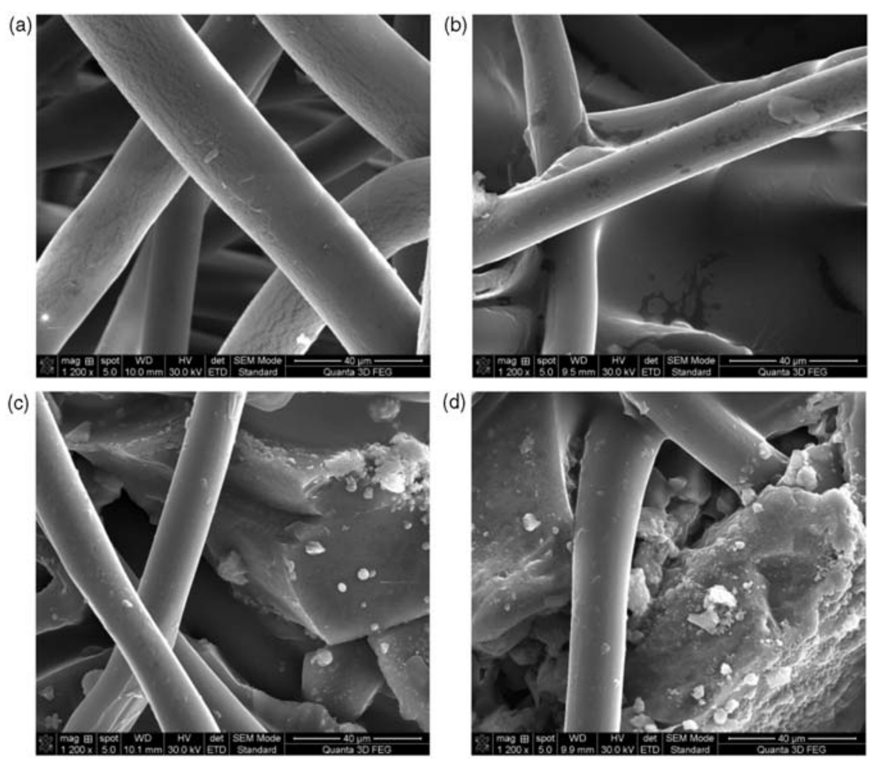

Figure 1. SEM images of the PLA meshes (a), PLA meshes after immersion in PVA solution (b), polymer/BG composite (c) and polymer/AgBG composite (d). PVA: polyvinyl-alcohol; PLA: poly-96 L/4D-lactide; SEM: scanning electron microscopy.

measuring the bioluminescence of the indicator strains with a bioluminescence imaging system XENOGEN-IVIS® Lumina from Caliper Life Sciences USA. Luria Bertani broth (LB) was prepared by dissolving yeast extract (5 g/L), tryptone (10 g/L) and NaCl (5 g/L) in distilled water, and autoclaving above 120°C. Soft and hard Luria Bertani agars (LA) were obtained by addition of 7.5 g/L agar and 15 g/L agar, respectively, to the same medium without NaCl. *Escherichia coli* and *Staphylococcus epidermidis* bacterial strains were stored in a glycerol broth suspension at –85°C. The strains were grown overnight at 37°C on hard LA plates and individual colonies were incubated in LB with vigorous shaking at 300 r/min. The cultures were diluted with LB to a proper optical density (OD_{600} 0.2–0.3) by adding 10 mL of LB in a sterile conical flask supplemented with ampicillin for *Escherichia coli* and with erythromycin for *Staphylococcus epidermidis*. Logarithmically growing cells were added to soft LA supplemented with appropriate antibiotic and gently mixed and poured onto hard LA plates supporting the samples. The conditions and the amount of the tested samples were similar for each bacterial strain. The time course of bioluminescent signal from light-emitting bacteria was examined for 24 h. The bioluminescence assay was performed every 2 h in triplicates in six-well plates, namely three control samples that are neat PLA meshes and three bioactive glass containing composites.

Results and discussion

The non-woven PLA meshes present large voids between the fibers (Figure 1(a)). After imersion in PVA solution, a thin film associated with PVA is evidenced between the PLA fibers (Figure 1(b)). Bioactive glass particles of both silver-containing and silver-free compositions appear as micrometric aggregates caught with PVA mainly between the PLA fibers (Figure 1(c) and (d)). The chemical composition of local areas was determined from EDS measurements performed on several sites of the composite samples corresponding to a mixed global composition, polymer component and bioactive glass component. The results are summarized in Table 1. The elemental composition of the analyzed areas, with respect to carbon and oxygen content, show for the composite samples that both PLA fiber and bioactive glass particles are covered with PVA.

The thermal analysis aimed to quantify the bioactive glass content in these composites based on their thermal degradation that is primarily related to the polymeric component.[23] The relative weight of the bioactive glass

Table 1. Elemental analysis results obtained from energy dispersive X-ray spectrometer (EDS) measurements

Elements (at %) →		C	O	Si	Ca	P	Ag
Sample ↓							
PLA	fiber	65.1	34.9				
PLA + PVA	global	65.9	34.1				
	fiber	87.7	12.3				
PLA + PVA + BG	global	63.6	31.2	2.0	2.8	0.4	
	fiber	78.1	19.2	0.6	1.7	0.4	
	glass	18.8	26.5	24.6	28.1	2.0	
PLA + PVA + AgBG	global	64.4	30.3	2.0	2.3	0.5	0.5
	fiber	76.1	22.9	0.4	0.4	0.1	0.1
	glass	47.4	23.3	5.8	21.4	1.0	1.2

PLA: poly-96 L/4D-lactide; PVA: polyvinyl-alcohol.

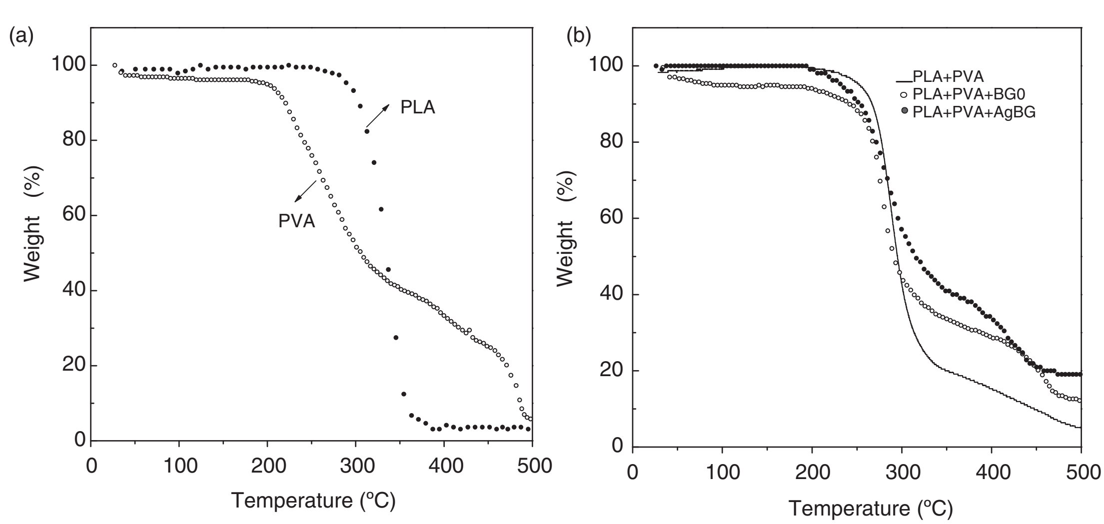

Figure 2. TGA curves of polymers (a) and composite samples (b). TGA: thermogravimetric analysis.

was estimated from the difference of the composites weight at the beginning and the end of each TG curve, as the polymer was assumed to be completely thermally degraded. In order to support this assumption, TG analysis was performed also on the two types of polymers used for the preparation of the composites.

By inspecting the TG run of PLA fiber (Figure 2(A)) a single sharp and intense weight loss of 97% is observed, and this is assigned to the decomposition of PLA.[24] The TG curve corresponding to neat PVA polymer (Figure 2(A)) shows three distinct weight loss steps related to the loss of trapped water and elimination reaction of hydroxyl side groups (200–300°C), a degradation stage (330–450°C) with elimination of residual acetate groups because of partially hydrolyzed PVA[25] dominated by chain-scission and cyclization.[26,27] The first degradation stage is associated with a weight loss of 60%, and the last two stages with 32% of weight loss. The initial molecular weight and the hydrolysis degree influenced the thermo-oxidative degradation of

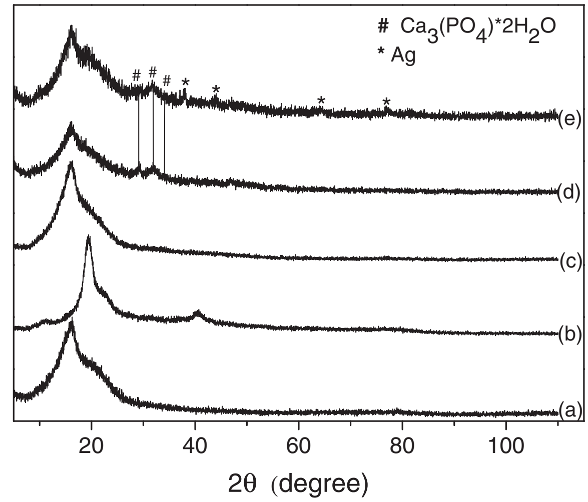

Figure 3. XRD patterns of (a) PLA, (b) PVA, (c) PLA + PVA, (d) PLA + PVA + BG and (e) PLA + PVA + AgBG composites. PLA: poly-96 L/4D-lactide; PVA: polyvinyl-alcohol; XRD: X-ray diffraction.

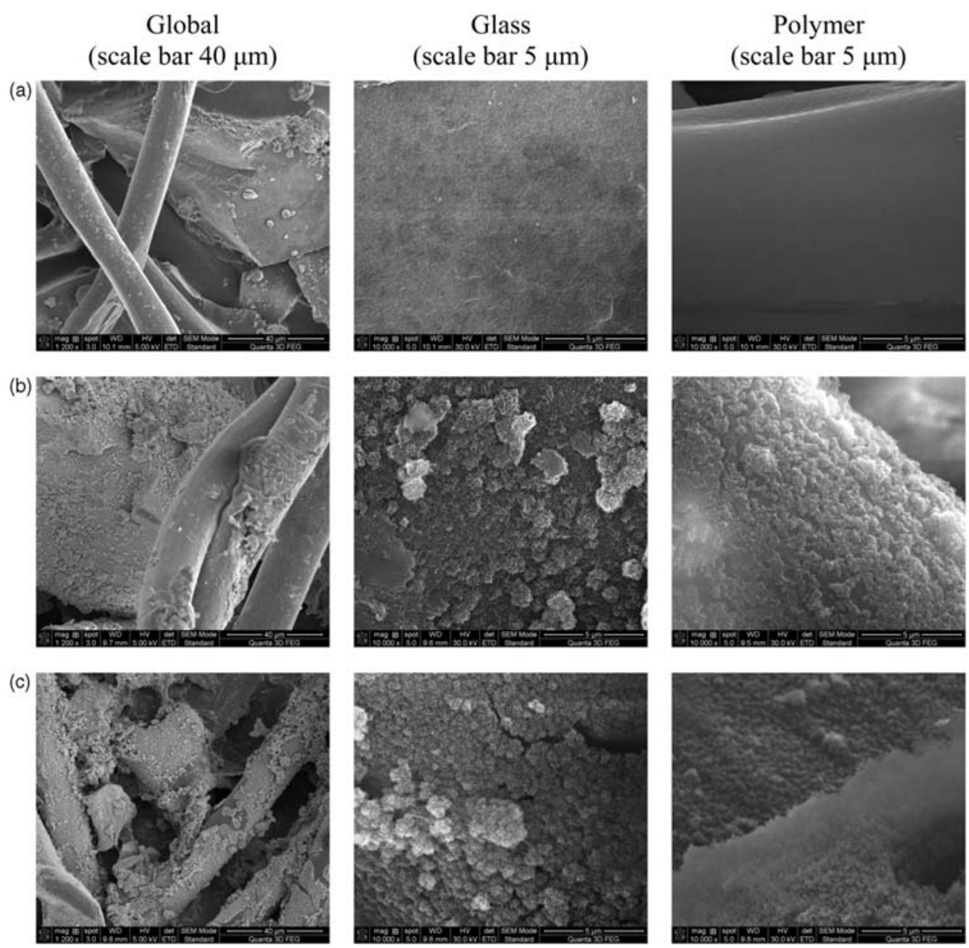

Figure 4. SEM images of polymer/BG composite prior to (a) and after incubation in SBF for 1 day (b) and 21 days (c). SEM: scanning electron microscopy; SBF: simulated body fluid.

PVA under dynamic TG conditions. Higher molecular weight causes greater complexity in the degradation process, whereas higher hydrolysis degree reduces the decomposition temperature of PVA.[28–30]

For PLA + PVA sample, a degradation pattern consisting of two stages can be observed (Figure 2(B)). The PVA degradation starts at a lower temperature than PLA degradation, for the PLA + PVA sample the degradation start temperature is in between, that is in agreement with the literature.[27] The weight percentage of bioactive glass content in the composites was found to be 6.5% BG and 14.7% AgBG, respectively, suggesting more adhesion of the silver containing glass to the polymer structure.

The X-ray diffractogram of PLA (Figure 3(a)) mainly consists of a broad line that reveals the amorphous phase, and a large peak at $2\theta = 16.4^\circ$ degree, typical for PLA.[31] The PVA polymer (Figure 3(b)) presents beside an amorphous broad line three large crystallization peaks at 11.2°, 19.4° respectively 40.5°, assigned to nanocrystalline domains.[32] The diffraction pattern given by the PLA + PVA polymer composite (Figure 3(c)) shows a broad diffraction peak centered at 16.4° just like the simple PLA sample. This result reflects the fact that the composite consists of a much higher PLA amount than PVA, in agreement with the preparation procedure. Some additional peaks characteristic to hydrated tricalcium phosphate $Ca_3(PO_4)_2{\cdot}2H_2O$[33] appear in the XRD pattern recorded from composite samples with bioactive glass (Figure 3(d) and (e)). Moreover, for the silver-containing bioactive glass composite, nanocrystalline metallic silver is also evidenced (Figure 3(e)). According to Scherrer formula, the crystallite sizes are close to 15 nm.

As proved by SEM analysis, already after first day of dynamic immersion in SBF on polymer meshes coated with BG and AgBG occur morphological changes implied by self-assembling of hydroxyapatite (HA) type crystals (Figures 4 and 5). In addition, silver chloride and silver phosphate crystals occur on AgBG containing composite after first day of immersion in SBF (Figure 5) as resulted from EDS analysis. These

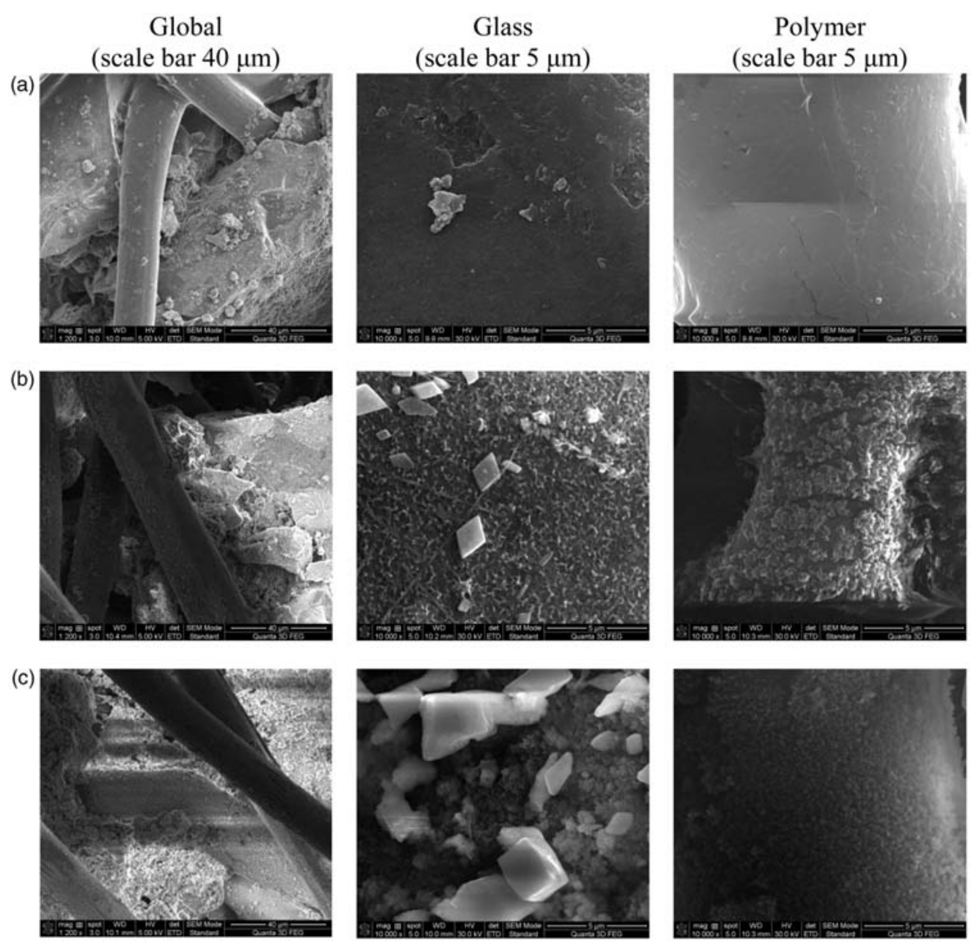

Figure 5. SEM images of polymer/AgBG composite prior to (a) and after incubation in SBF for 1 day (b) and 21 days (c). SEM: scanning electron microscopy; SBF: simulated body fluid.

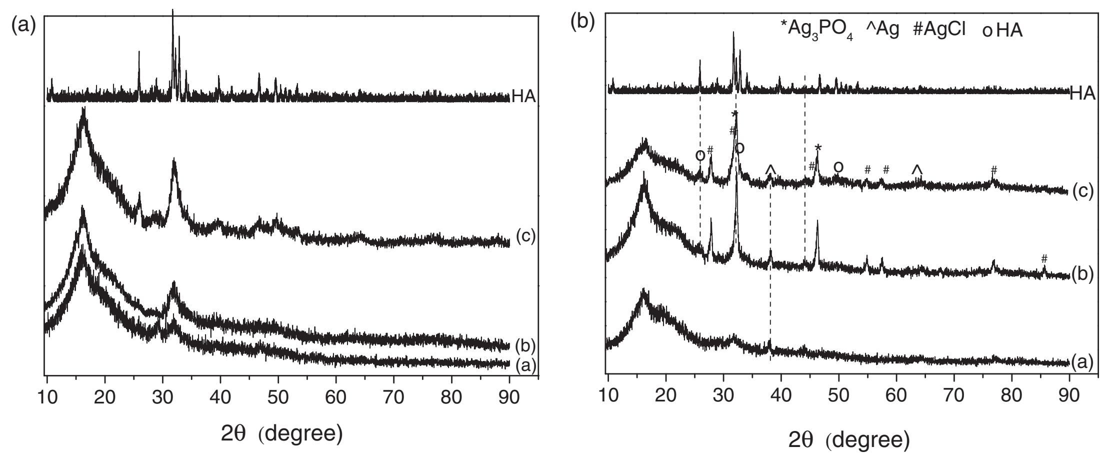

Figure 6. XRD patterns of (A) BG and (B) AgBG containing composites, (a) prior and after SBF soaking for (b) 1 day and (c) 21 days. XRD: X-ray diffraction; SBF: simulated body fluid.

Table 2. Elemental analysis results obtained from energy dispersive X-ray spectrometer (EDS) measurements carried out before and after incubation for 21 days in simulated body fluid (SBF)

Elements (at %) →	C	O	Si	Ca	P	Ag
Sample ↓						
PLA	65.1	34.9	0	0	0	0
PLA / SBF	65.4	34.6	0	0	0	0
PLA + PVA	65.9	34.1	0	0	0	0
PLA + PVA / SBF	65.9	34.1	0	0	0	0
PLA + PVA + BG	63.6	31.2	2.0	2.8	0.4	0
PLA + PVA + BG / SBF	53.1	33.5	0.1	8.6	4.7	0
PLA + PVA + AgBG	64.4	30.3	2.0	2.3	0.5	0.5
PLA + PVA + AgBG / SBF	54.2	32.1	0.6	7.2	4.2	1.7

PLA: poly-96 L/4D-lactide; PVA: polyvinyl-alcohol.

crystalline phases were identified also in the X-ray diffractograms (Figure 6(B) and (c)). The self-assembled AgCl nanocrystals and Ag_3PO_4 particles identified on the surface of silver-containing bioactive glass composite prove the release of silver ions into SBF that imparts antimicrobial properties.[18,34] Both SEM and XRD results show that the development of these crystalline phases does not inhibit the development of HA phase. As expected, the amount of HA phase increased with the immersion time (Figures 4 and 5). The high magnification SEM images as well as the results of EDS measurements (Table 2) prove that HA is formed not only on the bioactive glass component but also on the polymer fibers of the composites. At the same time, EDS data point out that there is no HA formation on neat polymer samples after immersion in SBF.

After first immersion day in SBF, the XRD results showed diffraction peaks characteristic for HA (Figure 6). The relatively narrow peaks indicate high crystallinity of the apatite formed in vitro at this early stage of immersion in SBF. The intensity of the apatite peaks increases with immersion time, suggesting the growth of HA type layer on the surface of the composites with bioactive glasses.

Both bioactive glass containing composites inhibited the bacterial growth (Figure 7). The time needed for bacterial growth inhibition depended on the bioactive glass composition. The effect also varied between bacterial species, *Escherichia coli* and *Staphylococcus epidermidis*, but no significant difference was seen between Gram-negative *Escherichia coli* and Gram-positive *Staphylococcus epidermidis* bacteria. The ability for inhibition of bacterial growth observed for the composite formed of PLA and PVA polymers and bioactive glass with SiO_2, CaO and P_2O_5 components without silver may appear somewhat surprising. According to earlier results reported on silver-free SiO_2-CaO-P_2O_5 bioactive glass system,[35] this glass system has neither bacteriostatic nor bactericidal effects on *Escherichia coli*. The bacterial growth inhibition effects, in this case, is related most likely to a certain hydrolysis degree of PVA.[36]

The silver-containing composite not only inhibited the bacterial growth but it had also bactericidal effect. This assessment is supported by the fact that the luminescent effect is proportional to the metabolism of the bacteria, and the quenching of the bacterial luminescence is a sign that they died. An increased luminescence was found initially (0 h moment) for BG composite sample (Figure 7), likely the bacteria recognized the presence of the sample and increased their metabolism.

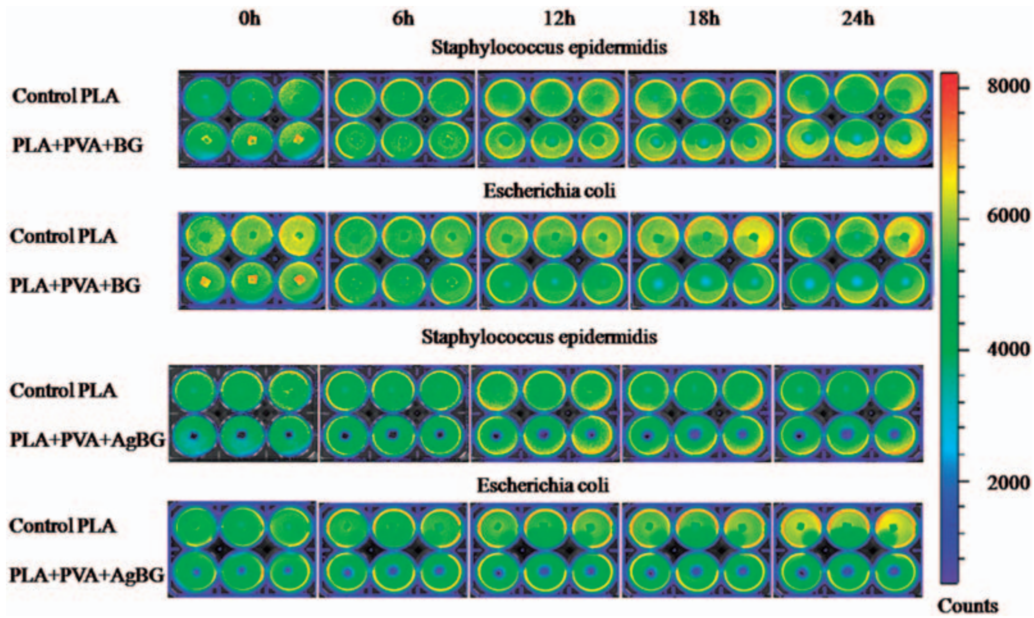

Figure 7. Bioluminescent signals from *Escherichia coli* and *Staphylococcus epidermidis* in response to the presence of polymer/BG and polymer/AgBG composites.

Conclusions

Non-woven poly-96 L/4D-lactide copolymer meshes loaded with silver containing and silver-free bioactive glass were obtained in PVA solutions by slurry dipping method under slow mechanical stirring. A higher adhesion to the polymer structure was evidenced for the silver-containing glass sample. HA type nanocrystals were self-assembled on polymer/glass composites already after first day of dynamic immersion in SBF. Both composites have tendency for high level of bioactivity according to their ability to form HAp at surface under in vitro conditions. With respect to silver-containing composite, due to the fact that Ag component could be potentially cytotoxic, the bioactivity could be properly appreciated after in vitro testing with cells in a future work. The PLA + PVA + AgBG composite contained nanocrystalline metallic silver and developed at interface with SBF AgCl and Ag_3PO_4 nanocrystalline particles. The tests on *Escherichia coli* and *Staphylococcus epidermidis* showed that silver-containing composite has bactericidal effect, but inhibitory effect on bacterial growth was proved also for the silver-free PLA + PVA + BG composite.

Funding

This research received no specific grant from any funding agency in the public, commercial, or not-for-profit sectors.

Acknowledgements

AV wishes to thank for the financial support provided from programs co-financed by The Sectoral Operational Programme Human Resources Development, Contract POSDRU 6/1.5/S/3 – "Doctoral studies: through science towards society". This work was accomplished in the framework of PNII Idei PCCE-129/2008 project granted by the Romanian National University Research Council – CNCSIS Romania.

Conflict of Interest

None declared.

References

1. Langer R and Vacanti JP. Tissue engineering. *Science* 1993; 260(5110): 920–926.
2. Dee KC, Puleo DA and Bizios R. *An introduction to tissue-biomaterial interactions*, 1st ed. New York: John Wiley & Sons, 2002.
3. Olsen-Claire J, Blaker JJ, Roether JA, et al. Bioglass® coatings on biodegradable poly(3-hydroxybutyrate) (P3HB) meshes for tissue engineering scaffolds. *Materialwiss Werkst* 2006; 37(7): 577–583.
4. Ignjatovic N and Uskokovic D. Synthesis and application of hydroxyapatite/polylactide composite biomaterial. *Appl Surf Sci* 2004; 238(1-4 spec iss): 314–319.
5. Boccaccini AR, Roether JA and Hench LL. Composites approach to tissue engineering. *Ceram Eng Sci Proc* 2002; 23(4): 805−816.
6. Suljovrujic E, Ignjatovic N and Uskokovic D. Gamma irradiation processing of hydroxyapatite/poly-L-lactide composite biomaterial. *Radiat Phys Chem* 2003; 67(3-4): 375–379.
7. Itoh S, Kikuchi M, Koyama Y, et al. Development of an artificial vertebral body using a novel biomaterial,

hydroxyapatite/collagen composite. *Biomaterials* 2002; 23(19): 3919–3926.

8. Niemela T, Kellomaki M and Tormala P. In vitro degradation of osteoconductive poly-L/DL-lactide/ β-TCP composites. *Key Eng Mater* 2004; 254–256: 509–512.
9. Niiranen N, Pyhalto T, Rokkanen P, et al. In vitro and in vivo behavior of self-reinforced bioabsorbable polymer and self-reinforced bioabsorbable polymer/bioactive glass composites. *J Biomed Mater Res A* 2004; 69(4): 699−708.
10. Jung Y, Kim S-S, Kim YH, et al. A poly(lactic acid)/ calcium metaphosphate composite for bone tissue engineering. *Biomaterials* 2005; 26(32): 6314–6322.
11. Hench LL JR, Jones JR and Sepulveda P. Bioactive materials for tissue engineering scaffolds. In: Polak JM, Hench LL and Kemp P (eds) *Future strategies for tissue and organ replacement*. London: Imperial College Press, 2002, pp.3–24.
12. Hoppe A, Guldal NS and Boccaccini AR. A review of the biological response to ionic dissolution products from bioactive glasses and glass-ceramics. *Biomaterials* 2011; 32(11): 2757–2774.
13. Bellantone M, Coleman NJ and Hench LL. Bacteriostatic action of a novel four-component bioactive glass. *J Biomed Mater Res* 2000; 51(3): 484–490.
14. Clupper DC and Hench LL. Bioactive response of Ag-doped tape cast Bioglasss® 45S5 following heat treatment. *J Mater Sci Mater Med* 2001; 12(10-12): 917–921.
15. Bellantone M, Williams HD and Hench LL. Broad-spectrum bactericidal activity of Ag_2O-doped bioactive glass. *Antimicrob Agents Chemother* 2002; 46(6): 1940–1945.
16. Simon V, Albon C and Simon S. Silver release from hydroxyapatite self-assembling calcium–phosphate glasses. *J Non-Cryst Solids* 2008; 354(15-16): 1751–1755.
17. Marambio-Jones C and Hoek EMV. A review of the antibacterial effects of silver nanomaterials and potential implications for human health and the environment. *J Nanopart Res* 2010; 12(5): 1531–1551.
18. Buckley JJ, Lee AF, Olivi L, et al. Hydroxyapatite supported antibacterial Ag_3PO_4 nanoparticles. *J Mater Chem* 2010; 20(37): 8056–8063.
19. Vulpoi A, Baia L, Simon S, et al. Silver effect on the structure of SiO_2-CaO-P_2O_5 ternary system. *Mater Sci Eng C* 2012; 32(2): 178–183.
20. Vulpoi A, Gruian C, Vanea E, et al. Bioactivity and protein attachment onto bioactive glasses containing silver nanoparticles. *J Biomed Mater Res A* 2012; 100A(5): 1179–1186.
21. Roether JA, Boccaccini AR, Hench LL, et al. Development and in vitro characterisation of novel bioresorbable and bioactive composite materials based on polylactide foams and Bioglass® for tissue engineering applications. *Biomaterials* 2002; 23(18): 3871–3878.
22. Kokubo T and Takadama H. How useful is SBF in predicting in vivo bone bioactivity? *Biomaterials* 2006; 27(15): 2907–2915.
23. Blaker JJ, Boccaccini AR and Nazhat SN. Thermal characterizations of silver-containing bioactive glass-coated sutures. *J Biomater Appl* 2005; 20(1): 81–98.
24. Ray SS and Bousmina M. Biodegradable polymers and their layered silicate nanocomposites in greening the 21st century materials world. *Prog Mater Sci* 2005; 50(8): 962–1079.
25. Alkan M and Benlikaya R. Poly(vinyl alcohol) nanocomposites with sepiolite and heat-treated sepiolites. *J App Polym Sci* 2009; 112(6): 3764–3774.
26. Brizzolara D, Cantow H-J, Diederichs K, et al. Mechanism of the stereocomplex formation between enantiomeric poly(lactide)s. *Macromolecules* 1996; 29(1): 191–197.
27. Yeh J-T, Yang M-C, Wu C-J, et al. Study on the crystallization kinetic and characterization of poly(lactic acid) and poly(vinyl alcohol) blends. *Polym Plast Technol Eng* 2008; 47(12): 1289–1296.
28. Popa M, Vasile C and Schneider IA. Thermoxidative degradation of poly(vinyl alcohol) under dynamic thermogravimetric conditions - I. Influence of heating rate and of molecular weight. *J Polym Sci Pol Chem* 1972; 10(12): 3679–3684.
29. Vasile C, Calugaru EM and Bodonea SF. Thermoxidative degradation of poly(vinyl alcohol) under dynamic thermogravimetric conditions - II. Influence of the hydrolysis degree. *J Polym Sci Pol Chem* 1981; 19(4): 897–905.
30. Vijayalakshmi SP and Madras G. Thermal degradation of water soluble polymers and their binary blends. *J Appl Polym Sci* 2006; 101(1): 233–240.
31. Zhou Z and Liu X. Fabrication of poly-l-lactide biomaterials with high mechanical properties using fiber oriented pressing. *J Macromol Sci B* 2008; 47(5): 847–858.
32. Bjorklund TG, Lim S-H and Bardeen CJ. The optical spectroscopy of poly(*p*-phenylene vinylene)/polyvinyl alcohol blends: from aggregates to isolated chromophores. *Synthetic Met* 2004; 142(1-3): 195–200.
33. Homaeigohar SS, Sadi AY, Javadpour J, et al. The effect of reinforcement volume fraction and particle size on the mechanical properties of β-tricalcium phosphate-high density polyethylene composites. *J Eur Ceram Soc* 2006; 26(3): 273–278.
34. Newby PJ, El-Gendy R, Kirkham J, et al. Ag-doped 45S5 Bioglass®-based bone scaffolds by molten salt ion exchange: processing and characterisation. *J Mater Sci Mater Med* 2011; 22(3): 557–569.
35. Balamurugan A, Balossier G, Laurent-Maquin D, et al. An in vitro biological and anti-bacterial study on a sol-gel derived silver-incorporated bioglass system. *Dent Mater* 2008; 24(10): 1343–1351.
36. Sedlarik V, Galya T, Sedlarikova J, et al. The effect of hydrolysis degree on the properties of antibacterial polymeric films based on poly(vinyl alcohol) and zinc sulphate for biomedical applications. *J Biomater Sci Polym Ed* 2010; 21(11): 1421–1440.